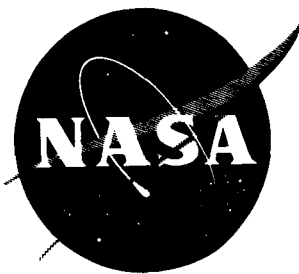


NASA TN D-94

NASA TN D-94

7N-37
195537
188



TECHNICAL NOTE

D-94

INVESTIGATION OF HIGH-SPEED IMPACT: REGIONS OF IMPACT
AND IMPACT AT OBLIQUE ANGLES

By James L. Summers

Ames Research Center
Moffett Field, Calif.

NATIONAL AERONAUTICS AND SPACE ADMINISTRATION

WASHINGTON

October 1959

(NASA-TN-D-94) INVESTIGATION OF HIGH-SPEED
IMPACT: REGIONS OF IMPACT AND IMPACT AT
OBLIQUE ANGLES (NASA. Ames Research
Center) 18 p

N89-70764

Unclas
00/37 0195537

TECHNICAL NOTE D-94

INVESTIGATION OF HIGH-SPEED IMPACT: REGIONS OF IMPACT
AND IMPACT AT OBLIQUE ANGLES

By James L. Summers

SUMMARY

Small metal spheres of widely varying densities were fired into copper and lead targets at velocities to 11,000 feet per second. Analysis of the high-speed results of the investigation indicates that the target penetration and cavity volume can be correlated as functions of the ratio of projectile to target density and of the ratio of impact velocity to speed of sound in target material. Impact for which the correlation equations apply is described as occurring in the fluid-impact region. This type of impact as well as other types is discussed. Penetration for impact at oblique angles is correlated with that for normal impact on the assumption that the component of velocity parallel to the target surface does not contribute to target penetration.

INTRODUCTION

A program of research directed toward the understanding of some of the details of high-speed impact is at present being conducted in the hypervelocity ballistic range of the Ames Research Center. The results of a preliminary portion of this investigation are reported in reference 1. In the reference report, a hydraulic analogy is used to describe the process of cavity formation during high-speed impact. Also presented in reference 1 is an equation suitable for engineering purposes giving the target penetration at impact velocities for which the hydraulic model is applicable. One purpose of the present report is to describe other types of impact and in doing so to amplify on this hydraulic or "fluid-impact region" as termed herein. A second purpose of the present report is to investigate the effects of impact at oblique angles and to examine the relationship between normal and oblique impact.

NOTATION

- c speed of sound in target material, the velocity of propagation of a plane longitudinal wave in a slender prismatic bar
- d diameter of spherical projectile

E	modulus of elasticity
m	mass of spherical projectile
p	penetration, measured from original target surface
V	impact velocity
v_P	volume of spherical projectile
v_T	volume of target cavity, measured from original target surface
θ	angle of obliquity of impact, measured between projectile flight path and line normal to target surface
ρ	mass density

Subscripts

N	normal to target surface
P	projectile
T	target

EXPERIMENTAL PROCEDURE

The tests were conducted by firing small spheres from a powder or light-gas gun into copper and lead targets at velocities to 11,000 feet per second. The spheres were made from various metals and alloys ranging from a magnesium-lithium alloy to a sintered tungsten compound, and varied in specific gravity from 1.5 to 17.1. The spherical models were mounted in supporting sabots which guided them down the bore of the gun barrel and provided protection from damaging effects of the propellant gases. After launch, the sabots were separated from the models and deflected aside and thereby were prevented from damaging the targets. Spark photographs of the projectiles were taken at numerous stations, and intervals of time and distance of flight between these stations were measured. The velocity as well as the physical condition of the projectiles in flight was determined from the above data. The targets were thick and massive compared to the cavities produced and, therefore, were considered representative of semi-infinite solids. A detailed description of the experimental apparatus employed and the data reduction techniques used is provided in reference 1.

RESULTS AND DISCUSSION

Fluid Impact

In reference 1, a fairly detailed description is given of the hydraulic model used to describe the type of impact for which data were presented. This description is, briefly, as follows. At very high speed, the dynamic pressure at impact $\left(\frac{1}{2} \rho_T V^2\right)$ is many times greater than the ultimate strength of either the projectile or target material and, as a consequence, both the projectile and the target behave as if they were fluids during the process of cavity formation. The material of the impacting body spreads over the crater and plates the interior of the target cavity. Such a plating process is illustrated in the photographs of figure 1 which show a sectioned portion of a copper target struck by a copper sphere. To illustrate the plating process more vividly, the sphere material has been lifted from the target delineating the interface between the impacting body and the target. As can be seen from the photographs, the surface of the cavity under the projectile material is quite smooth giving evidence of the plastic or fluid flow of the target during impact.

In connection with the plating phenomenon, it should be mentioned that the penetration data presented in reference 1 for copper spheres striking copper targets were obtained from measurements to the plated surface rather than to the interface. Measurement to the projectile-target interface in effect increases the penetration of copper spheres into copper targets with the result that these data are brought more into agreement with the data presented in reference 1 for spheres of materials other than copper striking copper targets. The re-evaluated copper into copper impact data are compared in figure 2 with data obtained from the impact of lead spheres into lead targets.¹ Plotted is the penetration in sphere diameters as a function of the ratio of impact velocity to speed of sound in the target, termed the "impact Mach number." The correlation of penetration on the basis of the impact Mach number and the limitations of this parameter are discussed in reference 1. The values for the speed of sound in the target materials were taken from reference 2 and are 11,670 feet per second and 4,025 feet per second for the copper and lead, respectively. The copper and lead data are seen from figure 2 to be in quite good agreement in contrast to the fair agreement obtained when penetration was measured to the plated face (cf. fig. 6, ref. 1).

¹For lead pellets striking lead targets, no corresponding interface could be found from examination of the craters produced. For the cases of impact of dissimilar materials, no difficulty was experienced in determining the proper cavity penetration and contour.

Examination of the data for lead impact presented in figure 2 reveals that for the data points plotted at impact Mach numbers of 1.50 and 1.69, the penetration is somewhat less than would be expected from extrapolation of the data obtained at the lower speeds. The spark photographs of the lead pellets in flight obtained when the tests were conducted indicate that for the low-speed data points, the lead pellets were spherical but that for the two high-speed points in question, the pellets were appreciably flattened in the direction of flight. The true pellet dimensions in the line of flight were determined from the spark photographs and the penetrations were recalculated on the basis of these dimensions. The flagged symbols in figure 2 show the corrected data, and the agreement of these points with those obtained at the lower speeds is evident. It appears that for correlation of penetration data, the pellet dimension to be used is that measured along the line of flight. Also, the necessity is demonstrated for employing good spark photographic equipment to determine the condition of the projectile prior to impact.

In addition to the above adjustments to the data of reference 1, certain other changes were made. Deleted were four data points obtained using spheres of nonmetallic materials and added were three data points for metal spheres impacting lead targets. Because of these several revisions to the original data, the correlation presented in reference 1 for the penetration of spheres of widely different densities into copper and lead targets was re-examined. The revised data of reference 1 are shown in figure 3(a) as a plot of penetration, in sphere diameters, as a function of the product of the impact Mach number and the ratio of the projectile to target density. The primary effect of the above changes was to reduce the scatter of the data. Also, the exponents of the impact Mach number and density ratio factors in the correlation equation were changed from 0.69 to $2/3$ to fit the revised data better. The revised correlation equation is:

$$\frac{p}{d} = 2.28 \left(\frac{\rho_P}{\rho_T} \right)^{2/3} \left(\frac{V}{c} \right)^{2/3} \quad (1)$$

Dependence of Cavity Volume on Kinetic Energy of Projectile

The results of a number of experimental investigations have shown that cavity volume is proportional to the kinetic energy of the impacting body (see ref. 3, for example). To explore this possibility, in reference 1, a relation between cavity volume and projectile kinetic energy

$\left(\frac{1}{2} mV^2 \right)$ was obtained by assuming the target cavity to be hemispherical

in shape with radius equal to the penetration. Cavity volume was then computed from the penetration equation presented in reference 1 and was given as

$$\left(\frac{\rho_T c^2}{2}\right) \left(\frac{2}{3} \pi p^3\right) = \text{const} \left(\frac{\rho_P}{\rho_T}\right) \left(\frac{mV^2}{2}\right) \quad (2)$$

with the quantity $(2/3)\pi p^3$ being the cavity volume. The interesting result that volume is proportional to the product of the density ratio and kinetic energy was noted in reference 1 but was not explained.

Subsequent to the publication of reference 1, the volumes of the target craters were measured. The analysis of the cavity volume data indicated that the volume varied as the $3/2$ power of the density ratio and the second power of the impact Mach number. The ratio of cavity volume to sphere volume is shown in figure 3(b) and, as can be seen, the volume data are adequately correlated for engineering purposes by the following equation:

$$\frac{v_T}{v_P} = 34 \left(\frac{\rho_P}{\rho_T}\right)^{3/2} \left(\frac{V}{c}\right)^2 \quad (3)$$

To compare the relation of the measured cavity volumes (eq. (3)) with that calculated in reference 1 (eq. (2)) from the penetration data, equation (3) was rewritten in terms of the projectile kinetic energy. Also introduced into equation (3) was the relation

$$E_T = \rho_T c^2$$

The rewritten volume equation is

$$v_T = 68 \left(\frac{\rho_P}{\rho_T}\right)^{1/2} \left[\frac{(1/2)mV^2}{E_T}\right] \quad (4)$$

It is of interest at this time to rewrite the penetration equation also in a similar manner giving

$$p = 3.56 \left(\frac{\rho_P}{\rho_T}\right)^{1/3} \left[\frac{(1/2)mV^2}{E_T}\right]^{1/3} \quad (5)$$

Note that equation (4) differs from equation (2) in that the exponent of the density ratio is $1/2$ instead of 1 . The reason for the difference is

that equation (2) was obtained on the assumption that the target craters were hemispherical whereas equation (4) was determined from reduction of the actual cavity volume data with the resulting change in exponent. The role played by the density-ratio factor is that of a cavity-shape parameter. For the case where the sphere and target are of the same material, the cavity produced by impact is very nearly hemispherical in shape. If the sphere material is much less dense than the target material, the cavity produced has the appearance of a broad but shallow spherical segment. Where the projectile material is much more dense than the target material, the cavity has a deep penetration compared to the crater radius at the target surface.

Regions of Impact

The hydraulic model describing impact is applicable only for impact occurring at sufficiently high speeds. With the thought that certain regions of impact could be defined, it was decided to explore impact at lower speeds where the strengths of the projectile and target would influence penetration. Accordingly, small spheres of tungsten carbide were fired into lead targets at speeds ranging from a few hundred to over 10,000 feet per second. The results are plotted in figure 4 as the penetration, in sphere diameters, as a function of the product of the impact Mach number and the ratio of projectile to target density. Representative target blocks were sectioned and photographs of the sections are shown above the portions of the graph to which they belong. As can be seen, three regions of impact are defined. At low velocities, the strength of the sphere's material is greater than the dynamic pressure of impact and the sphere penetrates the target as an undeformed projectile. The cavity produced is deep and narrow. In this region, the penetration varies as the $4/3$ power of the velocity as predicted from the DeMarre relation² (see ref. 4). With increase in velocity, a point is reached at which the impact pressure is sufficient to cause the tungsten-carbide sphere to fragment into a few large pieces at impact and the penetration ceases to follow the DeMarre relation. This is the beginning of a transition region of impact. As the impact velocity is increased further, the sphere shatters into numerous small pieces and the penetration actually decreases. Finally, a velocity is reached at which the typical fluid impact occurs, the crater formed is nearly hemispherical in shape, and the penetration is predicted by equation (1).

When impact occurs in the undeformed projectile region, penetration prediction can be made but the onset of transition cannot as yet be determined. Penetration in the fluid impact region cannot be predicted

²In the notation of the present report, the DeMarre relation is $p = \text{const } \rho_p^{2/3} v^{4/3}$ where the constant is empirically determined and is a function of the size and shape of the projectile as well as other physical and mechanical properties of both the projectile and target.

from impact occurring in the undeformed projectile region and the converse is also true. Within the transition region, the penetration can change with velocity in almost any fashion, depending on various physical and mechanical characteristics of the projectiles and targets. The exponent of the velocity factor can have a negative value, as seen from figure 4, or it can range up to some high value such as 1.4, as reported in reference 5.

The boundaries of the regions shown in figure 4 are applicable only to the one combination of pellet and target employed. For other combinations, the locations of the boundaries will be influenced by the physical and mechanical properties of the projectile and target materials as well as the impact velocity.

Effect of Target Strength

In connection with the above investigation, a very limited test was conducted to evaluate the effect of a change in one quantity, namely that of target strength, on penetration. For this test, 1/8-inch-diameter copper spheres were fired into hard and soft copper targets at speeds ranging from about 500 to 11,000 feet per second. The Brinell hardness numbers (10 millimeter ball and 500 kilogram load) of the hard and soft copper targets were 65 and 36, respectively. The penetration data obtained are plotted in figure 5. At an impact velocity of 600 feet per second, the penetration in the soft copper target is about 90 percent greater than that in the hard copper target. The craters produced at this velocity are virtually identical to the indentations made by a Brinell hardness testing machine and thus it might be expected that the relative penetrations could be determined from the Brinell hardness numbers. This is very nearly the case since an increase in penetration in the soft copper target of 80 percent over that of the hard copper target would be predicted from the Brinell hardness numbers. Examination of the target craters and recovered projectiles indicated that impact at this low velocity falls in the beginning of the transition zone previously mentioned.

At the impact velocity of 4,000 feet per second, the influence of target strength is greatly diminished since the penetration in the soft copper target is about 25 percent greater than that in the hard target. The impacts at this velocity are in the transition zone or at the beginning of the fluid-impact region.

With further increase in impact velocity, the effect of target strength continues to lessen and at 10,000 feet per second, the penetration in the soft copper is only 12 percent greater than that in the hard copper. Impact at this velocity is in the fluid impact region. An extrapolation of the data of figure 5 indicates penetration would be little affected by target strength at velocities of the order of 20,000 feet per second.

Oblique Impact

In addition to the previously described tests conducted with the target face normal to the projectile trajectory, firings were made with the targets at oblique angles. The targets were copper and the projectiles were 1/8-inch-diameter copper spheres. Examination of the cavities obtained from these tests indicated the penetration to decrease as the angle of obliquity was increased. Since the normal component of velocity also decreases with increase in angle of obliquity, the data were reduced by measuring the penetration normal to the target surface and computing the impact Mach number from the component of velocity normal to the target surface. In other words, it is assumed that the component of velocity parallel to the target surface does not contribute to the target penetration. The oblique-penetration data are compared with the normal penetration data in figure 6. The normal penetration data were obtained by varying the projectile velocity and the oblique penetration data were obtained by varying the target angle with a fixed projectile velocity of 7,000 feet per second in one case and 11,000 feet per second in the other. For the lower velocity the targets were of hard copper and for the higher velocity the targets were of soft copper. It is apparent that for both impact velocities, the oblique penetration correlates well with the normal penetration to a value for the angle of obliquity as great as 50° for the higher impact velocity. Shown in figure 7 are photographs of target craters, one for impact at an angle of 40° and the other for impact at 75° . The eccentricity of the crater is only slight at 40° , whereas at 75° , a distinctly elliptical cavity is observed. Where measurements were compared of the major and minor diameters (at the original target surface) of the craters produced at the two test velocities, it was found that for the same angle of impact, the eccentricity of the crater obtained at the higher impact velocity was significantly less than that for the lower velocity. It is of interest to note also that the Barringer crater in Arizona displays no eccentricity (it resembles a squared circle) when viewed from the air although the estimated angle of impact of the meteorite is about 45° . The results of the above observations suggest that if the impacting body is going fast enough, the crater formed will be circular regardless of the angle of impact. With regard to this point, many astronomers believe that the lunar craters, most of which are circular, were caused by meteoroids, the major fraction of which may have struck at oblique angles. The reason usually given for the round craters is that the explosive type impact resulting from the tremendous speed of the meteoroid would produce a circular crater for all but the most glancing angles of impact.

Evaluation of oblique impacts on the basis of the component of velocity normal to the target surface does not take into account all of the kinetic energy of the projectile. The remainder of the energy must go somewhere, perhaps in moving the cavity sideways or in spewing out the target material parallel to the target surface. The tests were not

conducted in sufficient detail to determine whether either of these occurred. Also, the small size of the cavities produced did not allow cavity volumes to be measured with accuracy.

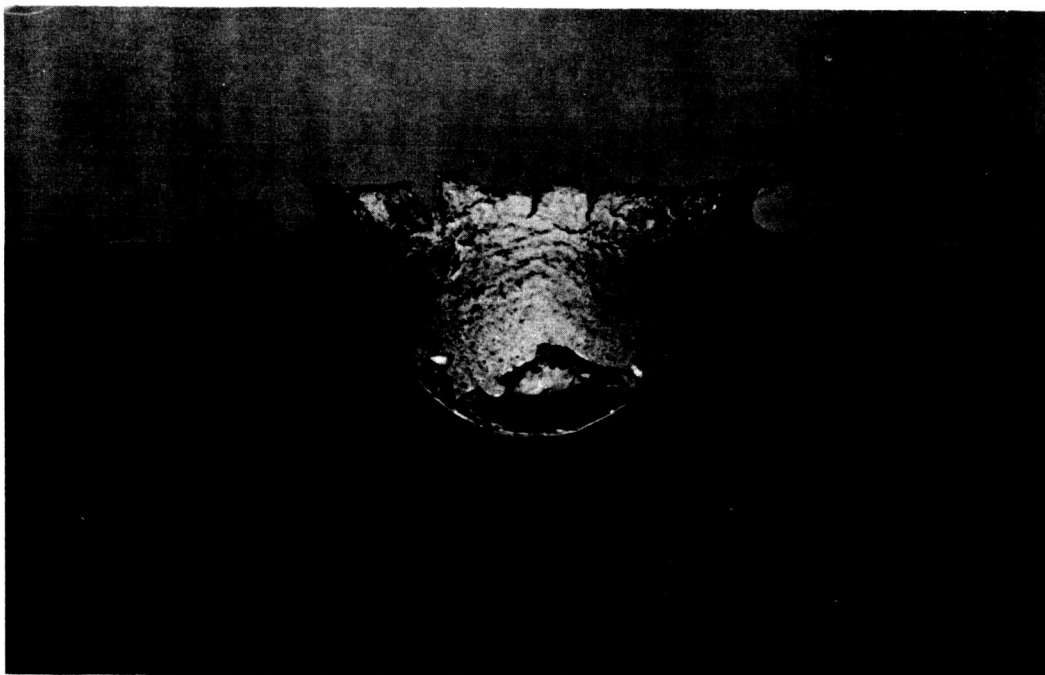
Ames Research Center

National Aeronautics and Space Administration

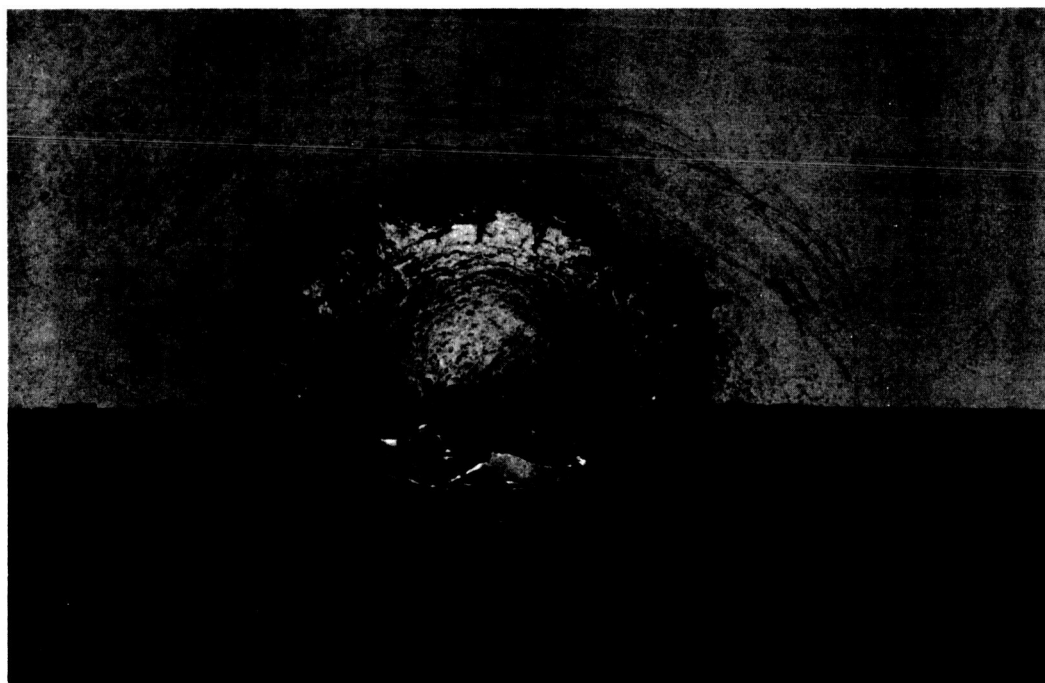
Moffett Field, Calif., July 28, 1959

REFERENCES

1. Charters, A. C., and Locke, G. S., Jr.: A Preliminary Investigation of High-Speed Impact: The Penetration of Small Spheres Into Thick Copper Targets. NACA RM A58B26, 1958.
2. Handbook of Chemistry and Physics, Fortieth ed., Chemical Rubber Publishing Company, 1958-1959, p. 2499.
3. Rinehart, J. S., and Pearson, J.: Behavior of Metals Under Impulsive Loads. The American Society for Metals, Cleveland, Ohio, 1954.
4. Cranz, C.: Lehrbuch der Ballistik. Vol. 1, Äussere Ballistik, Julius Springer, 1925, p. 465.
5. Huth, J. H., Thompson, J. S., and Van Valkenburg, M. E.: Some New Data on High-Speed Impact Phenomena. Jour. Appl. Mech., vol. 24, no. 1, Mar. 1957.



A-24726



A-24727

Figure 1.- Illustration of the plating effect for impact occurring in the fluid-impact region.

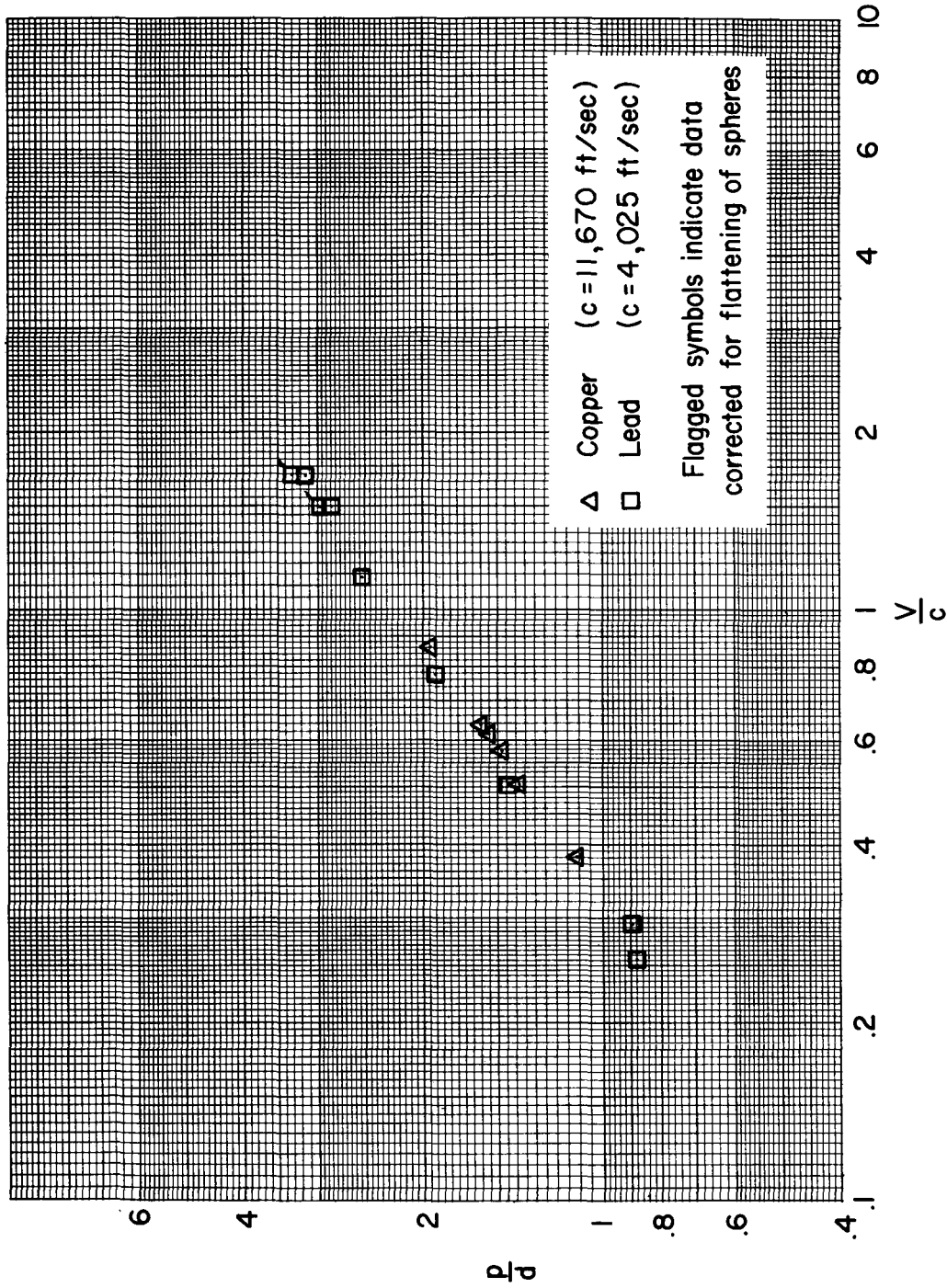
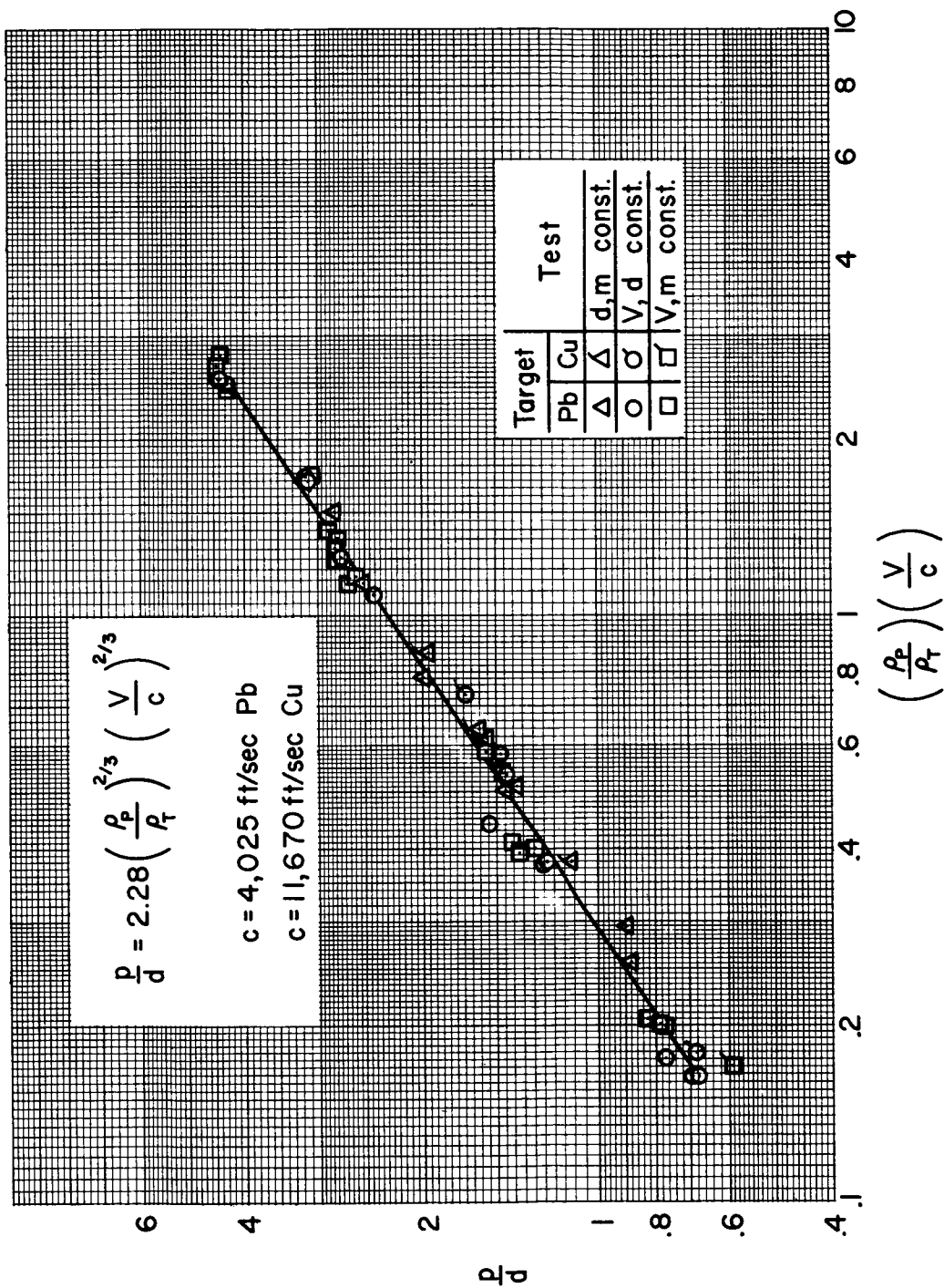
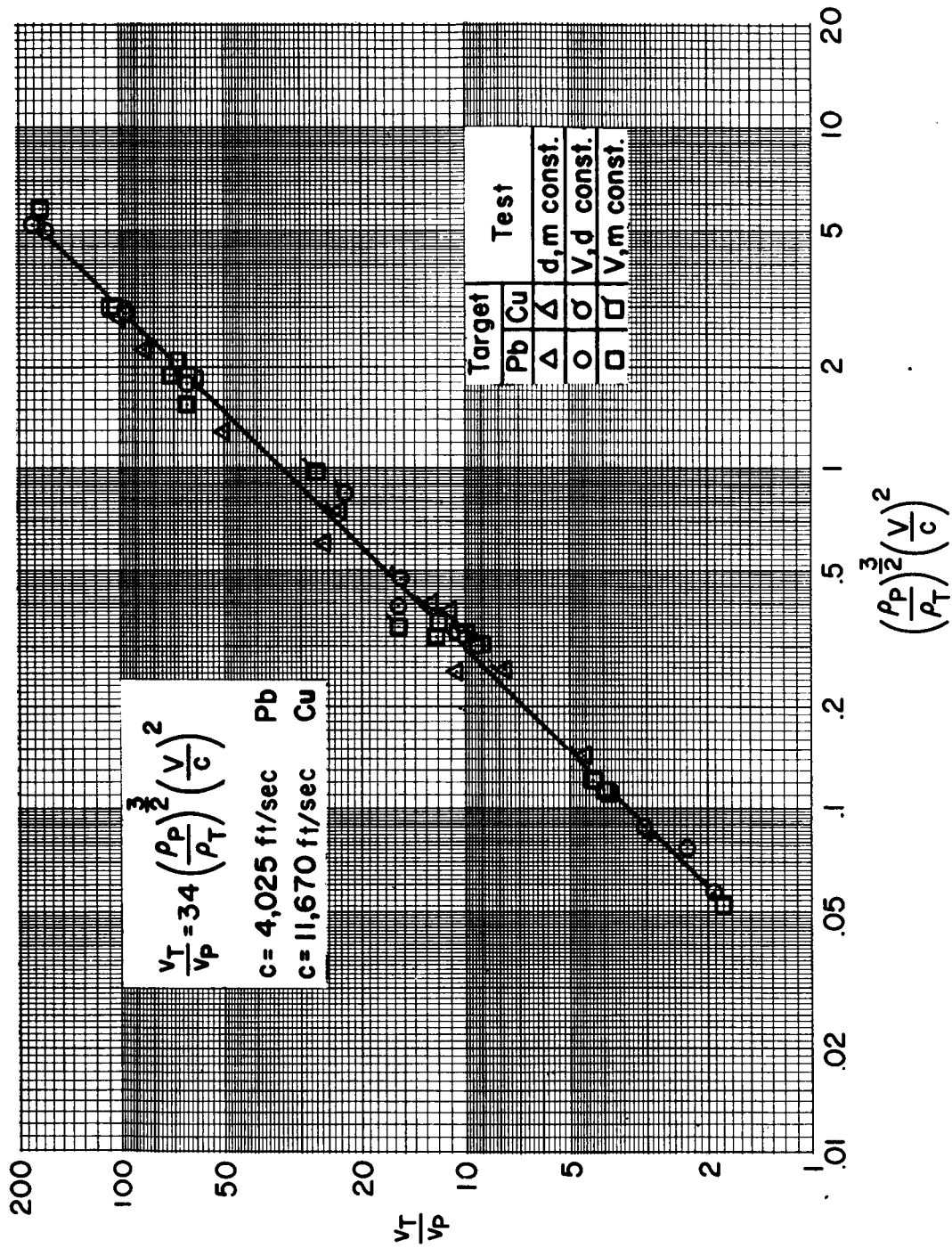


Figure 2.- Comparison of the penetration of copper spheres in copper targets and lead spheres in lead targets as a function of impact Mach number.



(a) Target penetration.

Figure 3.- Correlation of impact data.



(b) Cavity volume.

Figure 3.- Concluded.

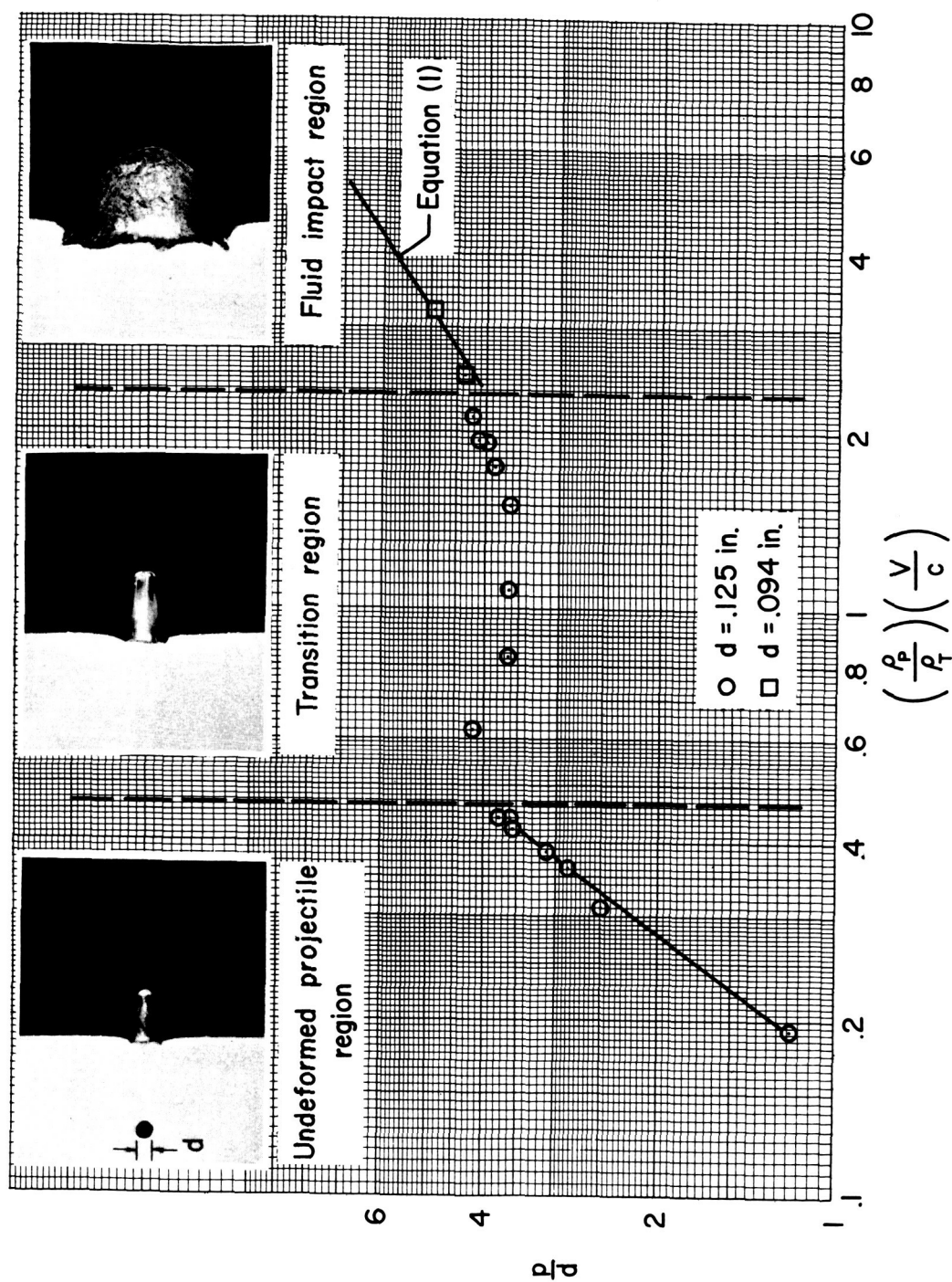


Figure 4.- The basic regions of impact for tungsten-carbide spheres impacting lead targets.

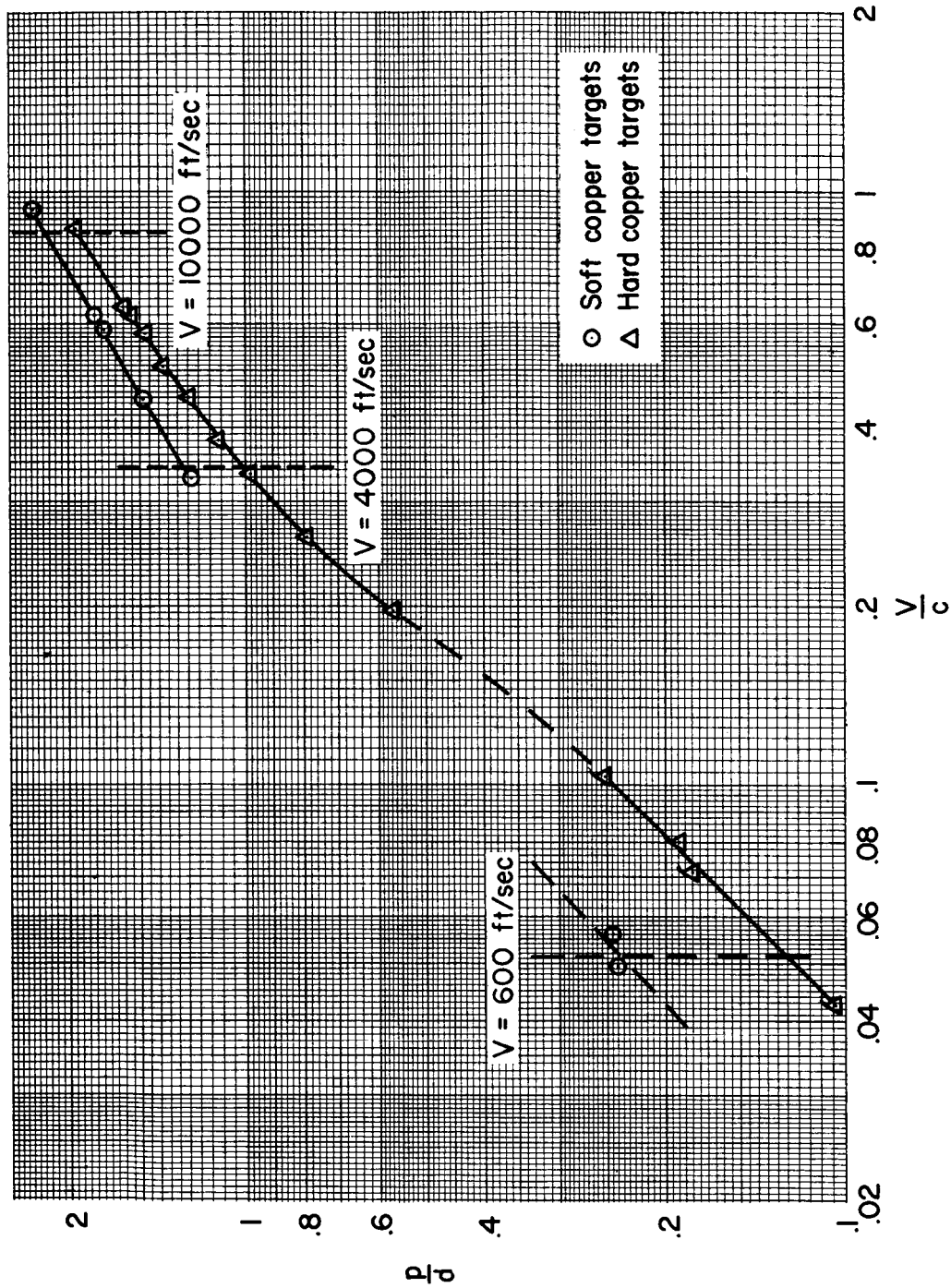


Figure 5.- Effect of target strength on penetration depth, 1/8-inch-diameter spheres of hard copper.

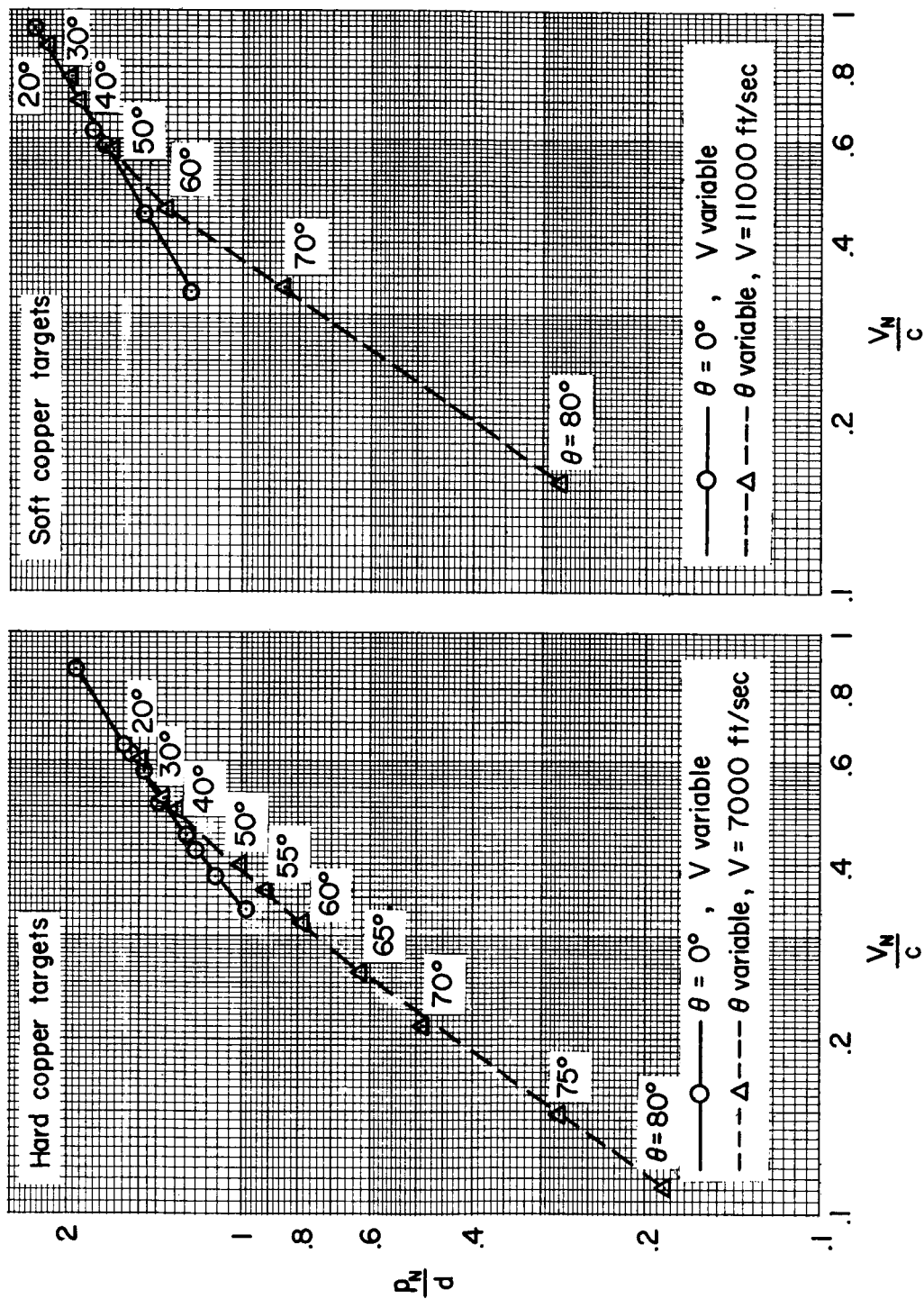


Figure 6.- Comparison of penetration for normal and oblique impact.



(a) $\theta = 40^\circ$

A-24851



(b) $\theta = 75^\circ$

A-24850

Figure 7.- Effect of angle of obliquity on crater shape,
 $V = 7000$ ft/sec.